CC BY

Heavy metal contamination in riverine systems: a comparative study of industrial vs. agricultural pollutants

Dr. Ravikant Kushwaha[1]; Siddharth Sriram[2]; Bodireddy Vamalatha[3]; Dr. Naresh Kaushik[4]; Dr. Ramesh Kumar V[5]; Prakash Ranjan Behera[6]; Ramachandran Thulasiram[7]

Received: 16 February 2025; Revised: 20 March 2025; Accepted: 05 April 2025; Published: 20 May 2025

Abstract

At five places, ambient sediments and water specimens were taken from the highest polluted river to analyze the pollution patterns of eight contaminants. Five sites along the river were selected due to their susceptibility to contamination from adjacent industrial operations. The tracking information, geo-accumulation indicator (Igeo), contaminating factor (CF), modified contamination degree (mCd), pollutant load indicator (PLI), and metal indicator (MI) were employed to conduct a comprehensive evaluation of contamination with heavy metals (HM). Two monitoring locations adjacent to the discharge sites of the Nanzih Export Processor Zone (NEPZ) had the highest contamination levels. The peak contamination periods for surface waters and sediment tests were 2020 to 2025. The surface water exhibited indications of HM pollution, with mCd exceeding 1.8. The HM features of the sediment specimen across the five years were analogous. This indicated that the naturally occurring attenuation mechanism was insufficient, necessitating the implementation of treatment technologies to enhance sediment cleanliness. This investigation establishes a foundation for thorough risk evaluations and cohesive management plans for the river's surface sedimentation and water condition. It would improve the inclusivity of assessments about HM pollution in worldwide rivers.

Keywords: Heavy metal, Contamination, Riverine, Agriculture, Industry**.**

1- Associate Professor, Maharishi School of Pharmaceutical Sciences, Maharishi University of Information Technology, Lucknow, Uttar Pradesh, India. Email: ravikant.kushwaha@muit.in, ORCID: https://orcid.org/0009-0006-2191-2000
2- Centre of Research Impact and Outcome, Chitkara University, Rajpura, Punjab, India.
Email: siddharth.sriram.orp@chitkara.edu.in ORCID: https://orcid.org/0009-0009-8776-1390
3- Centre for Multidisciplinary Research, Anurag University, Hyderabad, Telangana, India.
Email: bodireddyvamalathaaa@proton.me ORCID: https://orcid.org/0009-0004-3016-5444
4- Assistant Professor, uGDX, ATLAS SkillTech University, Mumbai, Maharashtra, India.
Email: naresh.kaushik@atlasuniversity.edu.in, ORCID: https://orcid.org/0000-0002-9896-4662
5- Associate Professor, Department of Biotechnology, Sathyabama Institute of Science and Technology, Chennai, India.
Email: rameshkumar.biotech@sathyabama.ac.in, ORCID: https://orcid.org/0000-0002-0310-1953
6- Assistant Professor, Department of Soil Science & Agricultural Chemistry, Institute of Agricultural Sciences, Siksha 'O' Anusandhan (Deemed to be University), Bhubaneswar, Odisha, India. Email: prakashbehera@sao.ac.in, ORCID: https://orcid.org/0000-0001-7068-272X
7- Professor, Department of Mechanical Engineering, Faculty of Engineering and Technology, JAIN (Deemed-to-be University), Ramanagara District, Karnataka, India. Email: t.ramachandran@jainuniversity.ac.in, ORCID: https://orcid.org/0000-0002-6991-0403
DOI: 10.70102/IJARES/V5I1/5-1-33

Introduction

Heavy Metal (HM) pollution can arise from renewable sources (Abramson *et al.*, 2024), such as weathering of rocks, or anthropogenic activity, including ore extraction, metal manufacturing, and applying fertilizers and pesticides in agriculture (Vij and Prashant, 2024; (Paul *et al.*, 2020). Human-caused metals exhibit increased mobility and bioavailability compared to their natural mineral counterparts, presenting heightened dangers to people and the environment (Chowdhury and Rahman, 2024; Mehdizadeh and Ravanshadniya, 2018). HM pollution has escalated markedly due to growing industrialisation (Adnan, Xiao, Zhao and Bibi, 2022). HMs emitted from diverse industrial operations ultimately contaminate the environment, particularly the surface waterways of urban regions. The study evaluated the pollution trend from HMs in global waterways from 1975 to 2020. Various regions exhibited distinct sources of HM pollution; extraction and production were recognized as the primary sources (Huy, D. T. N. 2018). The River is very contaminated, traversing a highly industrialized region and receiving effluents from multiple enterprises. The river collects effluents from various industrial areas, notably Renwu Industry Park, Dashe Industry Park, and Nanzih Export Processing Zones (NEPZ) (Yeh *et al.*, 2021). These industrial parks have numerous metal-based facilities, including metal surface processing and chip production facilities, which represent possible sources of contaminants for the waterway (Milošević *et al.*, 2022).

Before implementing more stringent environmental restrictions, the River exhibited significant HM pollution from unlawful discharges (Kumar *et al.*, 2024). The river's silt exhibited significant pollution, with copper (Cu) presenting the maximal mean content of 425.5 mg/kg dry weight. This amount is double the maximum levels established by many sediment quality criteria, including those of the Taiwan Ecological Protection Administration (TEPA) and the Canadian Council of Ministries of Ecology (CCME). The investigation was conducted briefly from 2018 to 2020, and the pollution patterns were not assessed. Studying the geographic and temporal contamination patterns with HMs is essential for conducting comprehensive environmental and health risk evaluation (Shi *et al.*, 2023).

Geographical and temporal trends were examined in many locations. For example, pollution from HMs exists, as well as sediments from the sea in river mouths and the coastlines of the southeastern region and on the southern coast of South Korea (Yang *et al.*, 2021). Their findings pinpointed primary pollution sources, variations in the spatial dispersion of HMs, and historical environmental shifts. These have established foundational information for efficient monitoring systems of pollution from HMs in the various regions.

This research comprehensively assesses the regional and seasonal pollution patterns from HMs in the Rivers from 2020 to 2025. In addition to the elevated levels of HMs in the top layer of water and particles, the research utilized the geo-accumulation indicator (Igeo), contaminated component (CF), altered degree of pollution (mCd), pollutant load indicator (PLI), and metal indicator (MI). Integrating individual evaluations (Igeo and CF) and synergistic evaluations of the eight contaminants will yield a more thorough understanding of the HM pollution status in the Rivers (Hoang *et al.,* 2021). Five sites along the river were selected due to their susceptibility to contamination from adjacent industrial operations. The sources of pollution were examined. The findings of this study will furnish a comprehensive foundation for forthcoming environmental and health-based risk evaluations, as well as the formulation of combined management plans for the river's top and sedimentary features (Feng *et al.,* 2023). The findings will aid in achieving Sustainable Development Goals (SDGs) and enhance the thorough assessment of HM pollution in worldwide rivers.

Methods

Study Area

The research area is 250 km², located on the southern floodplain of the upper Yellow River basin. The location of the soil is substantially influenced by outwash and penetration. Particulates of soil far from the Yellow River are comparatively finer. This region is located in a semi-arid or semi-humid moderate continental monsoon area, characterized by spring and winter shortages and fall and summer waterlogging (Wang and Zhang, 2024). The average temperature for the year is 15°C, and the mean annual sunlight duration is 2270.5 hours. The average yearly rainfall, which is distributed unevenly throughout the four seasons, is 630.5 mm. July typically experiences the highest monthly frequency of rainfall days (13.4 days) and the most precipitation (160.8 mm). The average daily rainfall is roughly 12.4 mm.

The study area encompasses the extensive Kaifeng urban region and its adjacent rural locales, characterized by concentrated manufacturing, farming, and residential zones. The water of the Yellow River serves various functions, including water supply, fish farming, industrial applications, domestic use, waste water management, and groundwater replenishment. HMs have been detected in the water diverting source, potentially endangering the wellness of the whole irrigation system. The predominant kinds of soil are muddy and sandy loam, originating from yellow fluvo-aquic soil characterized by a sandy loam consistency and elevated pH values. The principal irrigated crops in the region consist of maize, wheat, sorghum, soy products, rice, produce, and nuts. This region has an agricultural population that totals roughly 130k individuals. The Kaifeng urban area, characterized by a tiny population and diverse industries, is a sample study site comparable to cities in other emerging nations. The rapid expansion of agriculture and manufacturing has led to soil contamination from HM concentrations. The pollution of soil by HMs has surpassed its natural self-restoration potential. The harmful effects of metals have significantly compromised the framework and operation of soil ecology. Comprehending the hazards and origins of HM pollution in soil is essential for preserving a robust and environmentally friendly agricultural infrastructure.

Sampling and Analyses

- Layout of sampling sites and structure for sample collecting.

One hundred seven places for sampling were designated. They were disseminated uniformly across the study region. The sampling sites were chosen with meticulous attention to availability and spatial representation of the study area. The research area was delineated into homogeneous squares measuring 120 × 120 meters. Samples were extracted from the four sides and the middle of each square. To optimize sample participation, the five specimens collected from every square were amalgamated and regarded as a single specimen for that particular square. Every specimen was obtained from a soil layer 0-25 cm thick, with coarse debris eliminated, and every specimen weighed around one kg.

- Analysis of the collected specimen.

Every specimen was air-dried in the lab before pulverized with an inflatable rod. The specimens went through a 1 mm nylon filter, thoroughly mixed, and spread uniformly on plastic sheets. Twenty g specimens were taken from around 50 random sites. The extracts were further pulverized until they could traverse a 0.25 mm nylon sieve.

Graphite oven Atomic Absorption Spectra (AAS) were employed to ascertain calcium amounts. In contrast, nuclear absorption using flames was utilized to measure chromium, nickel, copper, zinc, and lead levels. Oxidation gasification-atomic fluorescent spectroscopy was employed to ascertain the concentrations of Hg and As. National benchmark sample soils have been included in the breakdown and evaluation procedure for quality assurance. Every ingredient utilized in the analytical method was a certified reagent. The water used was highly pure (sub-boiled water). The duplication collection ratio was maintained at 12%-16% to maintain sample quality, and the recuperation rate met the analytical quality assurance standards.

Methodologies for Research

The research objectively assessed the risk and identified HM contamination. Nemerow, Geo-accumulation, and Hakanson's ecological danger indices were employed to evaluate geographically pollution levels and possible risks associated with HM levels. Pearson's correlation factor and principal component research were utilized to ascertain the statistical correlation of HM similarity. The next step involved integrating spatial and statistical studies to evaluate the dangers and origins of pollution by HMs. The workflow is illustrated in Figure 1.

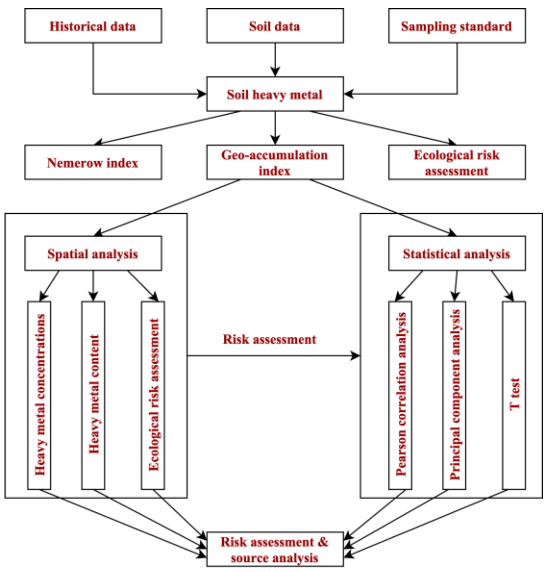

Figure 1: Flowchart of risk assessment & source analysis.

Results

Density of HMs in Surface Water Specimens

All analyzed contaminants were identified in the water specimen across the five years (2020-2025) and at the five sampling areas (L1–L5), as illustrated in Fig. 2. Cu, Pb, Ni, Zn, and Cr were the predominant components across all regions and periods. These are prevalent HMs in several manufacturing and producing sectors, including metal surface treatment, wrapping, and chemical. The investigation employed Positive Matrix Factorizations (PMFs) to ascertain the likely causes of pollution from HMs in the river, concluding that the factories along its shoreline were the primary contributors. The study indicated that pollution from HMs in the river resulted from the prevalence of metal-based production activity in the adjacent factory areas. The sewage effluents are likely sources of pollution from HMs in the river.

The HM signatures for the sites were analyzed and correlated with their possible origins. The L1 and L2 fingerprints exhibited dissimilarities, suggesting distinct sources of pollution. L1 was adjacent to Dashe Economic Park, which hosts numerous plastics producers and electroplating facilities. This explains the elevated amounts of Zn and Cd in L1 compared to other places. L2 was situated adjacent to industry, which has numerous petrochemical and a few metal-related enterprises, representing possible sources of metal pollution. L3 and L4, situated downward, exhibited analogous fingerprints, indicating that the pollution in both locations originated from comparable sources.

Most HMlic substances, such as Cr, Cu, Pb, Ni, and Hg, exhibited the maximal levels in L3 and L4 adjacent to the discharge locations NEPZ. The NEPZ contains semiconductor packaging and metal surface treatment facilities, which discharge sewage containing HMs. L1 and L2, situated upstream, had distinct fingerprints compared to L3 and LA, indicating that the influence of pollution with HMs from upstream sources was negligible. This is attributed to reduced levels of metals at L1 and L2. L5, situated downriver, exhibited analogous indicators to L3 and L4, suggesting downstream metal pollution from L3 and L4. The pollution at L3 and L4, characterized by elevated levels, influenced the HM levels at L5.

All HM levels, except Ni, peaked between 2020 and 2022. The mean HM levels in L3 have the strongest favorable connection ($p < 0.01$) with the mean levels for those years. The sewage outflow from NEPZ constituted a substantial source of HM pollution in the Rivers in 2020 and 2022. The patterns in HM concentrations fluctuated across the five years. This results from unlawful releases, yearly precipitation, or alterations in production operations. Deriving comprehensive inferences regarding the patterns based solely on how they concentrated proved challenging.

Compared to the TEPA irrigated guidelines, the highest amounts of HMs yearly were below permissible levels, excluding Pb in 2021 (1.7 times greater) and Hg in 2021 and 2023 (2.1 and 3.7 percent). Compared to the freshwater toxicity accepted, Cu and Pb readings for every year exceeded the limit by 3.5 to 57.6 times. This signifies potential for enhancement in discharge control.

Drawing definitive inferences regarding the synergistic pollution levels and trends from data collected during monitoring proved challenging. This was achieved through the utilization of mCd. Combining mCd data with threshold values yields precise evaluations of metal pollution levels and patterns.

Evaluation of HM Pollution Patterns in Groundwater

Standard deviations for HMs are suggested based on multiple criteria to determine mCd. Because the river provides water for agricultural purposes, the research used standard metrics for irrigation water quality.

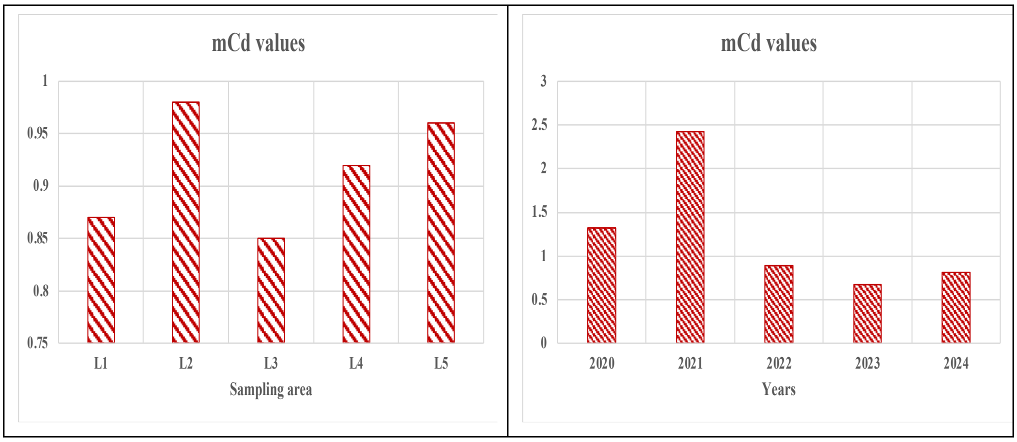

Figure 2: Spatial and temporal mCd analysis in surface water.

The mCd results indicate no significant variations in the regional pattern of water pollution at the sites, as illustrated in Figure 2a. The concentrations of HM contaminants in the water at all five specimen sites were the minimum limit levels (mCd = 1.6). The findings were congruent with the PLI score. At all sample sites, Hg exhibited the most positive association with mCd levels ($p < 0.03$), where Ni, Cd, and Cr had a significant favorable relationship with mCd values ($p < 0.03$). Moreover, Hg and Pb exhibited substantial associations with mCd level at L5 ($p < 0.03$). Mercury, lead, nickel, cadmium, and chromium affect water quality.

The temporal pattern of pollution oriented on mCd levels was as follows. While five of the nine HMs exhibited peak concentrations in 2022 according to mCd values, 2021 recorded the most significant level of HM synergy pollution (mCd = 2.4). The contents in the water were 2-9 times greater in 2021 compared to their baseline levels than in 2022. Except in 2021, surface water's yearly HM pollutants were less than the minimum limit levels (mCd = 1.6). The PI values were congruent with these findings. This suggests that the water is polluted and is unsuitable for irrigation. Measures to diminish HM density, including regulating outflow conditions before dumping into the Riverbed and implementing on-site solutions like wetland technological advances, should be employed to enhance the water condition.

Density of HMs in sediment specimens

Cu, Ni, Cr, Pb, and Zn exhibited relatively elevated quantities. The stages of HMs in sediment typically exceed those in water due to their propensity to form precipitates, collect, and adhere firmly to particles. Analogous to HM levels in the surface water specimens, most HMs exhibited the highest levels in L3 and L4, whereas L5 recorded the lowest amounts. The amount of HMs in sediments did not show the same trend as that in the surrounding water. The association among HM contents in public water and sediments was low, with a Pearson correlation of ≤ 0.56 ($p < 0.02$). This suggests that the amount of HMs in soil is influenced not only by the present level in water at the surface but additionally by previous concentrations due to settling, buildup, and adsorption.

The river's inherent attenuation mechanism is insufficient; therefore, local governments must implement measures to enhance water quality, such as enforcing rigorous discharge rules, imposing harsher penalties, and conducting sediment remediation efforts. L3 exhibited the strongest connection ($p < 0.02$) with the mean HM content in the soil tests throughout the years, indicating that L3 was the primary contributor to HM pollution.

At every sampling area, the concentrations of Cd, Cu, Ni, and Zn exceed the upper threshold of the TEPA's condition of sediment standard and the Effect Range Mean (ERM) determined by the National Oceanographic and Meteorological Agency (NOMA) by a factor of 1.2 to 5.8. Other heavy elements, including arsenic, chromium, lead, and mercury, were of lesser significance, exhibiting quantities below the upper threshold of the established criteria.

These monitoring data could not determine the extent of pollution and the complementary evaluation of HM contamination in the sample soils. The review indices Lgeo, CF, mCd, PLI, and MI were utilized to analyse separate and combinatorial pollution of metals. The pollution trends of contaminants in sedimentary specimens were analyzed using the following indices.

Assessment of HM Pollution Patterns in Sediment

The individual evaluation uses Igeo and the impact component. The Igeo was utilized to assess a specific HM in the sand specimens quantitatively. In contrast to monitoring information, the individual indices account for the baseline levels of HMs. Most HMs exhibited peak Igeo values at L3 and L4, whereas L5 recorded the lowest. Cadmium exhibited the highest Igeo levels across all sample locations, excluding L4, with other sites demonstrating moderate to substantially polluted levels of cadmium. Simultaneously, all regions exhibited uncontaminated traces of As, Cr, and Hg, with Igeo values less than zero. Most HMs exhibited their peak Igeo levels in the most recent period of 2023-2024. This signifies the density of HMs in the soil. For example, 2024 exhibited significantly elevated levels of cadmium, whereas 2023 displayed modestly elevated levels of copper.

The findings on the temporal and spatial distributions of Igeo values align with the evaluations of geographical and temporal patterns determined by CF values. Measures and methods to enhance sediment excellence, including washing, thermal removal, and bioremediation, are imperative and urgent. The authorities must work swiftly to improve the sediment content of the River. Alongside the particular indices, mCd and PLI were utilized to furnish a more thorough assessment of HM pollution.

The combined evaluation utilizes the altered level of pollution measure, the Pollutant Load Indicator (PLI), and the Metal Indicator (MI). The mCd indicator was used to evaluate the pollution of the analyzed pollutants in the sediments. The mean mCd value across five areas was 7.2, signifying that the sand specimen from the River exhibited medium to severe contamination. The PLI score across the five test sites indicated the sediment condition was compromised (PLI = 2.3).

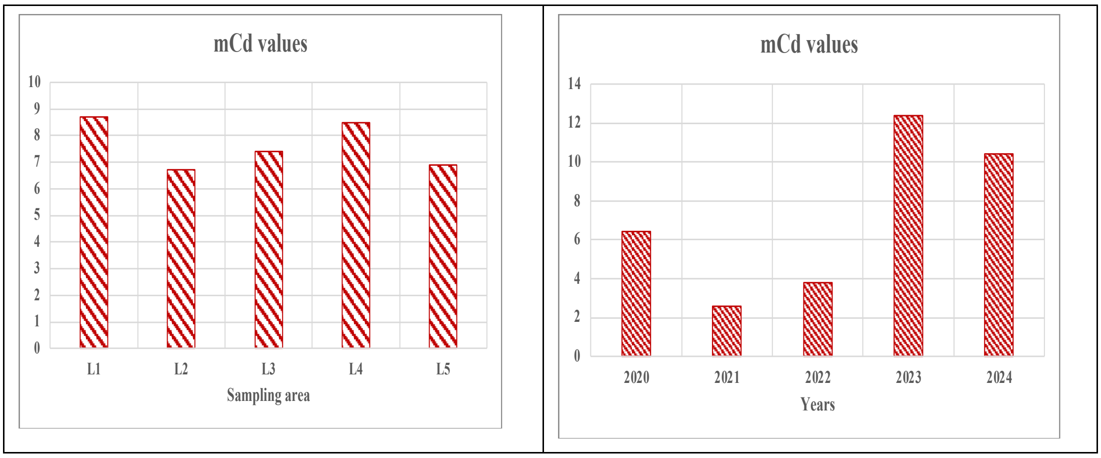

Figure 3: Spatial and temporal mCd analysis in sediment.

Figure 3a illustrates the regional trends. L4 exhibited a maximum mCd score of 8.6, signifying substantial contamination by HMs. L5 exhibited a minimum mCd of 5.2, indicating a moderately to significantly contaminated condition. The PLI calculations showed that L4 exhibited the most significant HM pollution. At all sampling locations, Cd exhibited the most critical positive connection with mCd ($p < 0.03$). This verifies that cadmium was the HM troubling the River, and reducing the amount present in discharge streams must be prioritized.

The temporal pattern of mCd and PLI scores exhibited a consistent downward order: 2023 > 2024 > 2020 > 2022 > 2021 (Fig. 3 b). In 2023 and 2024, mCd levels fluctuated between 8 and 16, signifying substantial silt contamination throughout both years. The mCd readings for sediments from 2020 to 2022 exhibited moderate to severe contamination by metals. The deposits exhibited contamination with metals, as shown by mCd and PLI values. The amount of HMs in sediment specimens is demonstrated by physical reactions (such as adhesion, evaporation, and complexation), biological absorption, and environmental variables (including hurricanes and heavy rainfall). These mechanisms would influence the seasonal patterns of contaminants in the sediment collections.

Alongside the mCd and PLI indices, MI was employed to evaluate the HM content levels of the sediment according to the higher limit scores established by TEPA's particle quality standard. The mean MI value throughout the five years at different locations was 9, signifying a significant degradation in sediment integrity.

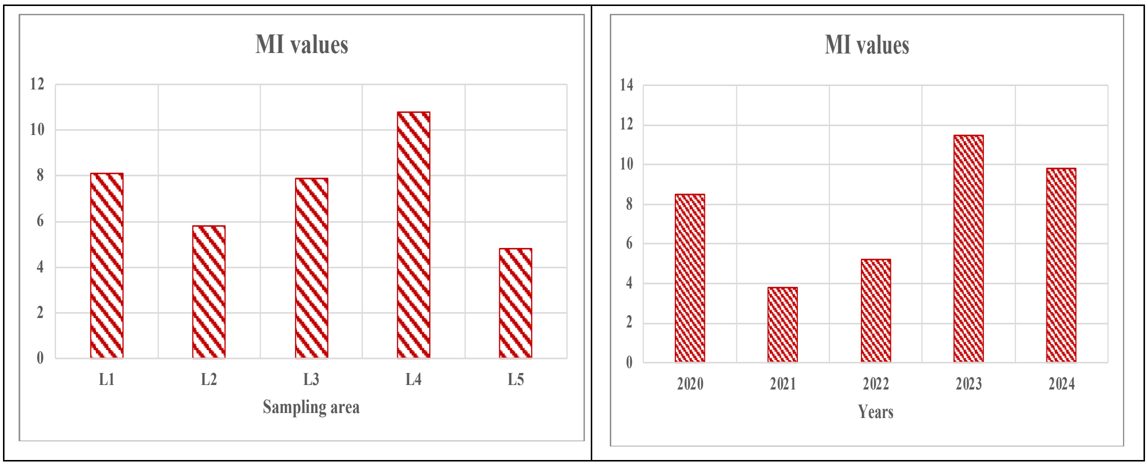

Figure 4: Spatial and temporal metal index analysis in sediment.

As illustrated in Figure 4, the regional and temporal patterns corresponded well with the mCd indices. The soil characteristics for L1, L3, and L4 were categorized as severely impacted, while L2 and L5 were significantly affected. 2021 was classified as impacted; 2020, 2023, and 2024 were designated as considerably affected, while 2022 was deemed strongly afflicted by HM pollution. This revealed that, according to the higher thresholds of quality of sediment standards, HMs in the rock samples had polluted and adversely impacted sediment integrity. The sand quality of the River requires immediate enhancement.

In conclusion, the River exhibited indications of significant HM pollution, particularly in its sediments. Urgent and essential measures are required to purify and safeguard the water from rivers and silt, particularly when the water is utilized for upstream agriculture. These initiatives must be sustainable and aligned with the SDGs. To safeguard the well-being of people, irrigation utilizing water should be halted as a last resort. Ecological management organizations must rigorously regulate sewage from manufacturing facilities to ensure compliance with requirements before discharge, and unauthorized discharges should incur harsh penalties. Constant water and soil condition tracking and regular assessment of wastewater discharge norms must be rigorously enforced. On-site restoration methods, including wetland technological advances, chemical treatments, and digging, should be implemented to enhance sedimentary and water quality and save aquatic life. Additionally, proposals and implementations must be advanced to balance all three innovative city features.

Conclusion

The tracking information was utilized to assess HM pollution in the uppermost and subsurface sediments of the River, situated in a highly industrialized region. Copper, lead, nickel, zinc, and chromium were the five predominant metals in the water and soil specimens from the River. Most contaminants exhibited peak densities and mCd levels at L3 and L4, near the discharge locations of the NEPZ.

The surface water exhibited indications of HM pollution. The presence of HM concentration in the soil tests was concerning. The HM content profiles of the sediment over five years were comparable, indicating that the natural abatement mechanism was insufficient to remediate the deposits. Short- and long-term remedial techniques to improve surface sediment and water health are essential. The findings will serve as a crucial foundation for recommending measures to enhance sedimentary and water excellence, and for subsequent research on environmental and healthcare risk assessments related to toxic HMs in the Rivers.

References

Abramson, J., Adler, J., Dunger, J., Evans, R., Green, T., Pritzel, A., Ronneberger, O., Willmore, L., Ballard, A.J., Bambrick, J. and Bodenstein, S.W., 2024. Accurate structure prediction of biomolecular interactions with AlphaFold 3. *Nature, 630*(8016), pp.493-500.

Adnan, M., Xiao, B., Xiao, P., Zhao, P. and Bibi, S., 2022. Heavy metal, waste, COVID-19, and rapid industrialization in this modern era—Fit for sustainable future. *Sustainability*, *14*(8), p.4746. https://doi.org/10.3390/su14084746

Chowdhury, F. N., and Rahman, M. M. 2024. Source and Distribution of Heavy Metals and Their Effects on Human Health. In Heavy Metal Toxicity: Human Health Impact and Mitigation Strategies (pp. 45-98). *Cham: Springer Nature Switzerland.*

Feng, W., Deng, Y., Yang, F., Miao, Q. and Ngien, S.K., 2023. Systematic review of contaminants of emerging concern (CECs): distribution, risks, and implications for water quality and health. *Water*, *15*(22), p.3922. https://doi.org/10.3390/w15223922

Hoang, H.G., Lin, C., Chiang, C.F., Bui, X.T., Lukkhasorn, W., Bui, T.P.T., Tran, H.T., Vo, T.D.H., Le, V.G. and Nghiem, L.D., 2021. The individual and synergistic indexes for assessments of heavy metal contamination in global rivers and risk: A review. *Current Pollution Reports*, *7*, pp.247-262.

Huy, D. T. N. 2018. Risk Level of Viet Nam Telecommunication Industry under Financial Leverage during and After the Global Crisis 2007-2009. *International Academic Journal of Innovative Research, 5*(1), 77–90. https://doi.org/10.9756/IAJIR/V5I1/1810008

Kumar, R., Goyal, M. K., Surampalli, R. Y., and Zhang, T. C. 2024. River pollution in India: exploring regulatory and remedial paths. *Clean Technologies and Environmental Policy*, *26*(9), 2777-2799.

Mehdizadeh, H., and Ravanshadniya, M. 2018. Technical and economic assessment of building performance through light metal frame (LSF). *International Academic Journal of Science and Engineering*, *5*(1), 211–221. https://doi.org/10.9756/IAJSE/V5I1/1810019

Milošević, A., Grubić, A., Cvijić, R., Čelebić, M., and Vuković, B. 2022. Control Factors of Iron Mineralization in the Metallogeny of the Ljubija Ore Region. *Archives for Technical Sciences*, *1*(26), 13–22. https://doi.org/10.7251/afts.2022.1426.013M

Paul, P., Ripu Ranjan Sinha, R.R.S., Aithal, P.S., Aremu, P.S.B. and Saavedra M, R., 2020. Agricultural informatics: an overview of integration of agricultural sciences and information science. *Indian Journal of Information Sources and Services*, *10*(1), pp.48-55. https://doi.org/10.51983/ijiss-2020.10.1.2832

Shi, J., Zhao, D., Ren, F. and Huang, L., 2023. Spatiotemporal variation of soil heavy metals in China: The pollution status and risk assessment. *Science of the Total Environment*, *871*, p.161768. https://doi.org/10.1016/j.scitotenv.2023.161768

Vij, P. and Prashant, P.M., 2024. Analyzing Soil Pollution by Image Processing and Machine Learning at Contaminated Agricultural Field. *Natural and Engineering Sciences*, *9*(2), pp.335-346. https://doi.org/10.28978/nesciences.1575484

Wang, Y. and Zhang, Q., 2024. Distribution characteristics of drought and flood hazards in northern China against the background of climate warming. *Natural Hazards*, *120*(7), pp.5987-6009.

Yang, L., Ma, X., Luan, Z. and Yan, J., 2021. The spatial-temporal evolution of heavy metal accumulation in the offshore sediments along the Shandong Peninsula over the last 100 years: anthropogenic and natural impacts. *Environmental Pollution*, *289*, p.117894. https://doi.org/10.1016/j.envpol.2021.117894

Yeh, G., Lin, C., Nguyen, D. H., Hoang, H. G., Shern, J. C., and Hsiao, P. J. 2021. A five-year investigation of an industrially affected river's water quality and heavy metal mass flux. *Environmental Science and Pollution Research, 1-8.* https://doi.org/10.34133/2021/7189376